Supplementary Information

Maxwell G. De Jong, Kevin B. Wood

1 Backward Master Equation Operator

The master equation operator Ω is populated from Markovian transition rates that come from the dynamics allowed in our system within the Moran framework. We denote $T^+[x_i]$ as a transition that increases the number of mutants in microhabitat x_i. Explicitly, our three transition rates increasing the number of mutants from an initial state (j, k, ℓ) are

$$\begin{aligned} T^+[x_0](j,k,\ell) = &\underbrace{(N-j)}_{\text{WT dies}} \underbrace{\frac{(N-j)r_0(x_0)}{(N-j)r_0(x_0)+jr^*(x_0)}}_{\text{Pick WT}} \underbrace{\mu}_{\text{WT mutates}} \\ &+ \underbrace{(N-j)}_{\text{WT dies}} \underbrace{\frac{jr^*(x_0)}{(N-j)r_0(x_0)+jr^*(x_0)}}_{\text{Pick mutant}} \underbrace{(1-\beta)}_{\text{No migration}} \\ &+ \underbrace{(N-j)}_{\text{WT dies}} \underbrace{\frac{kr^*(x_1)}{(N-k)r_0(x_1)+kr^*(x_1)}}_{\text{Pick right mutant}} \underbrace{\beta}_{\text{Migration}} \end{aligned} \tag{S1}$$

$$\begin{aligned} T^+[x_1](j,k,\ell) = &\underbrace{(N-k)}_{\text{WT dies}} \underbrace{\frac{(N-k)r_0(x_1)}{(N-k)r_0(x_1)+kr^*(x_1)}}_{\text{Pick WT}} \underbrace{\mu}_{\text{WT mutates}} \\ &+ \underbrace{(N-k)}_{\text{WT dies}} \underbrace{\frac{kr^*(x_1)}{(N-k)r_0(x_1)+kr^*(x_1)}}_{\text{Pick mutant}} \underbrace{(1-2\beta)}_{\text{No migration}} \\ &+ \underbrace{(N-k)}_{\text{WT dies}} \underbrace{\frac{jr^*(x_0)}{(N-j)r_0(x_0)+jr^*(x_0)}}_{\text{Pick left mutant}} \underbrace{\beta}_{\text{Migration}} \\ &+ \underbrace{(N-\ell)}_{\text{WT dies}} \underbrace{\frac{\ell r^*(x_2)}{(N-\ell)r_0(x_2)+\ell r^*(x_2)}}_{\text{Pick right mutant}} \underbrace{\beta}_{\text{Migration}} \end{aligned} \tag{S2}$$

and

$$T^+[x_2](j,k,\ell) = \frac{N-\ell}{(N-\ell)r_0(x_2)+\ell r^*(x_2)}[(N-\ell)r_0(x_2)\mu + (1-\beta)\ell r^*(x_2)] + \frac{N-\ell}{(N-k)r_0(x_1)+kr^*(x_1)} k r^*(x_1)\beta \quad \text{(S3)}$$

Within the Moran process, we also have transitions that decrease the number of mutants in a given microhabitat. We denote $T^-[x_i]$ as the transition decreasing the number of mutants in microhabitat x_i. The explicit transition rates are given by

$$T^-[x_0](j,k,\ell) = \underbrace{j}_{\text{Kill mutant}} \underbrace{\frac{(N-j)r_0(x_0)}{(N-j)r_0(x_0)+jr^*(x_0)}}_{\text{Choose WT}} \underbrace{(1-\beta-\mu)}_{\text{WT grows without mutation or migration}} + \underbrace{j}_{\text{Kill mutant}} \underbrace{\frac{(N-k)r_0(x_1)}{(N-k)r_0(x_1)+kr^*(x_1)}}_{\text{Pick WT}} \underbrace{\beta}_{\text{Right migration}} \quad \text{(S4)}$$

$$T^-[x_1](j,k,\ell) = \underbrace{k}_{\text{Kill mutant}} \underbrace{\frac{(N-k)r_0(x_1)}{(N-k)r_0(x_1)+kr^*(x_1)}}_{\text{Choose WT}} \underbrace{(1-2\beta-\mu)}_{\text{WT grows without mutation or migration}} + \underbrace{k}_{\text{Kill mutant}} \underbrace{\frac{(N-j)r_0(x_0)}{(N-j)r_0(x_0)+jr^*(x_0)}}_{\text{Pick WT}} \underbrace{\beta}_{\text{Left migration}} + \underbrace{k}_{\text{Kill mutant}} \underbrace{\frac{(N-\ell)r_0(x_2)}{(N-\ell)r_0(x_2)+\ell r^*(x_2)}}_{\text{Pick WT}} \underbrace{\beta}_{\text{Right migration}} \quad \text{(S5)}$$

and

$$T^-[x_2](j,k,\ell) = \underbrace{\ell}_{\text{Kill mutant}} \underbrace{\frac{(N-\ell)r_0(x_2)}{(N-\ell)r_0(x_2)+\ell r^*(x_2)}}_{\text{Choose WT}} \underbrace{(1-\beta-\mu)}_{\text{WT grows without mutation or migration}} + \underbrace{\ell}_{\text{Kill mutant}} \underbrace{\frac{(N-k)r_0(x_1)}{(N-k)r_0(x_1)+kr^*(x_1)}}_{\text{Pick WT}} \underbrace{\beta}_{\text{Left migration}} \quad \text{(S6)}$$

With these transition rates, Ω is populated according to

$$\Omega_{m,n} = \begin{cases} W^{n\to m} & n \neq m \\ -\sum_{m'\neq m} W^{n\to m'} & n = m \end{cases} \quad \text{(S7)}$$

where $W^{n\to m}$ is the transition rate from initial state n to final state m. Note that the number of mutants can change by one at most, so the backwards master equation operator is sparse.

We can then solve the mean first passage time equation

$$-1 = \sum_{m' \neq m_f} T(m_f|m')\Omega_{m',m_i} \tag{S8}$$

where $T(m_f|m_i)$ is the mean time required for a system initially in state m_i to first reach state m_f. All of the natural boundary conditions are already imposed by Ω, but we do need to specify that

$$T((n^*(x_0), n^*(x_1), n^*(x_2))|(n^*(x_0), n^*(x_1), n^*(x_2))) = 0 \tag{S9}$$

for any initial state $(n^*(x_0), n^*(x_1), n^*(x_2))$, which is intuitively obvious.

2 Characterization of Intermediate Regime

To further investigate evolution in the intermediate regime, where heterogeneity can either speed or slow fixation, depending on the specific profile, we calculated the minimum and maximum fixation times (τ_f^{min} and τ_f^{max}, respectively) as δs is modulated to create different selection pressure distributions (Fig. S1a). While in many cases the fixation time is decreased by only a few percent, we do find larger effects in the high and low migration limits (i.e. on the edges) of the intermediate regime. To understand how the spatial τ_f profiles change over this intermediate region, we fix μ and traverse across a trajectory in β as shown by the arrow in Fig. S1a. As we increase β, τ_f smoothly transitions from being minimized at $\delta s = 0$ to being maximized near $\delta s = 0$ (Fig. S1b).

3 Alternative Landscape Parameters

The results in the main text were all generated with $\langle s \rangle = 0.167$. However, the existence of three regions of parameter space is not specific to this particular value of $\langle s \rangle$. In Fig. S2, we see that we observe three regions of parameter space with a variety of values for $\langle s \rangle$. It is worth noting that the relative size and location of the intermediate region change with $\langle s \rangle$, and the magnitude of effects also changes with $\langle s \rangle$. However, the existence of these regions is constant throughout these different classes of landscapes.

Note that it a second intermediate region appears with larger values of $\langle s \rangle$. The existence of this additional intermediate region does not follow the same intuitive understanding and is more subtle. This second intermediate region arises due to numerical reasons. Upon discretizing our selection landscape in steps of $\Delta\delta s = 0.1$, it is possible for the "true" minimum to occur near $\delta s = 0$ but not exactly at this value. With these relatively large step sizes, it allows the "true" minimum to be mapped to $\delta s = 0$ even though the true minimum

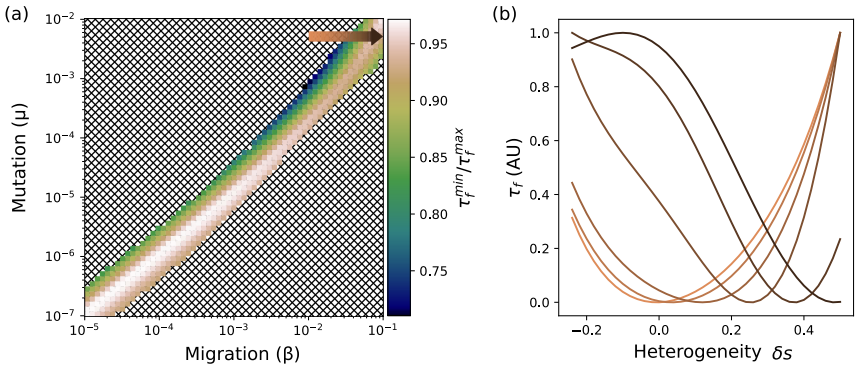

Figure S1: (a) Minimum fixation times (τ_f^{min}) over different selection pressure distributions (relative to the maximum fixation times, τ_f^{max}) in the intermediate parameter region where fixation can be both accelerated and decelerated. $N = 25$ and $\langle s \rangle = 0.167$. (b) Across a specific trajectory in the intermediate region (arrow in panel (a)), the dependence of τ_f on heterogeneity (δs) transitions smoothly from a state with a minimum at $\delta s = 0$ (light test curve) to one with a maximum at $\delta s = 0$ (darkest curve). For ease of comparison, fixation times are scaled to arbitrary units between 0 and 1.

occurs at some small non-zero value. So the apparent area between the two intermediate regions is actually an artifact of the numerical discretization of our landscape. Further evidence comes from looking at the fixation times in this second intermediate region, which differ by less 1% from the spatially homogeneous landscape, so it is likely of little significance.

We can also vary N to confirm that the existence of the three regions of parameter space is resilient to changes in N. We investigated a few different values of N in Fig. S3, and we again see the same three regions of parameter space.

4 Alternative Topologies

We can also confirm that the existence of three regions of parameter space is not predicated upon the specific topology chosen. The results of the main text assumed a nearest-neighbor connection without migration between the boundary microhabitats. We can easily imagine additional topologies for a specified selection landscape. We can remove one of the existing connections and allow migration between the boundary microhabitats (which is equivalent to cyclically permuting the selection landscape with the same connections). The resulting phase plot is shown in Fig. 4(a). We can also imagine a global topology in which all microhabitats are connected to all others. The phase plot from this global topology is shown in Fig. 4(b). Note that the phase plots differ quantitatively when the topology is changed, but all three topologies support three different

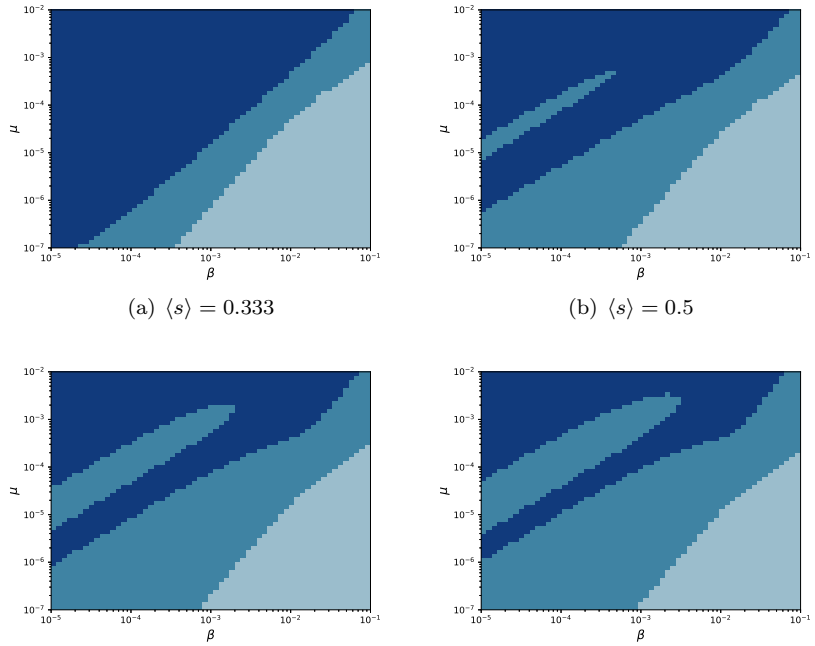

(a) $\langle s \rangle = 0.333$ (b) $\langle s \rangle = 0.5$

(c) $\langle s \rangle = 0.667$ (d) $\langle s \rangle = 0.833$

Figure S2: Changing $\langle s \rangle$ does not change the existence of three regions of our parameter space. The appearance of a second intermediate region is artificial and due to numerical discretization.

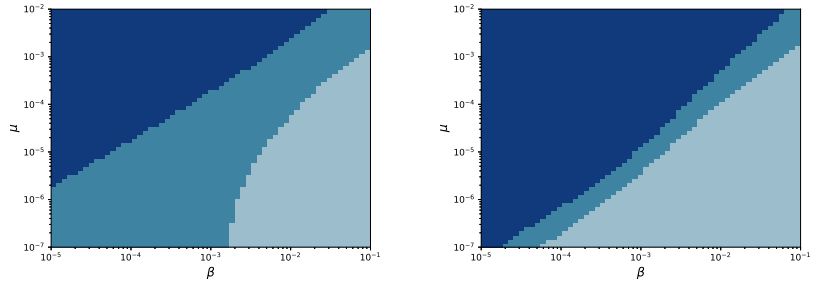

(a) $N = 15$ (b) $N = 35$

Figure S3: Different population sizes N result in the same qualitative behaivor.

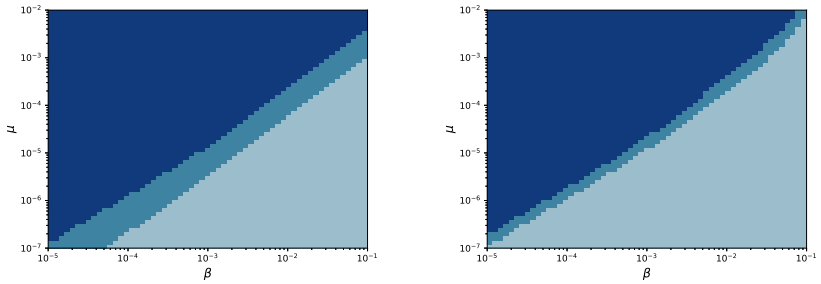

(a) Permuted Topology (b) Global Topology

Figure S4: Different topologies also produce three unique regions of parameter space.

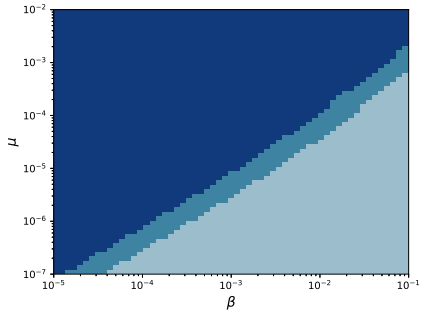

Figure S5: A monotonic selection landscape produces a qualitatively similar phase plot to that generated with a non-monotonic landscape.

regions of parameter space.

5 Monotonic Landscape

We can also imagine using a monotonic selection landscape. A non-monotonic landscape potentially allows for more complicated dynamics due to the lack of a single direction of selection pressure gradient. In Fig. S5, we see that a monotonic landscape also results in three regions of parameter space. Future work will be focused on understanding the role of monotonicity on the fixation times.

6 Analytical Approximation for Single Habitat

In a single microhabitat with selection pressure s, we can approximate the fixation time $\tau_f(s)$ in the limit $\mu \ll 1$ as

$$\tau_f(s) \approx \frac{1}{\lambda_{eff}} = \frac{1}{\mu N P_{fix}(s)}. \tag{S10}$$

Equation S10 provides a good approximation to $\tau_f(s)$ for a range of $\mu \ll 1$ (Figure S6). This approximation assumes that mutations are sufficiently rare that fixation times are dominated by arrival and fixation of a single mutant (i.e. the timescale of fixation of a single mutant is fast compared to the expected arrival time of the next mutant via mutation). Therefore, the arrival time distribution is exponential with a rate parameter λ_{eff}. The factor μN is the transition rate $T^+(0)$ for increasing the number of mutants by one starting from zero mutants (see, for example, Equation S1 with $j = 0$ and $\beta = 0$). P_{fix} is the probability of fixation of a single mutant in a habitat with selection pressure s and no mutation. The expression for $P_{fix}(s)$ is well-known, but for completeness, we briefly repeat the derivation here. To do so, we first write an iterative equation for p_i, the probability of fixation from a starting condition of i mutants. We have

$$\begin{aligned} p_i &= T^-(i)p_{i-1} + T^+(i)p_{i+1} + (1 - T^+(i) - T^-(i))p_i \\ &= \frac{\rho}{1+\rho}p_{i-1} + \frac{1}{1+\rho}p_{i+1} \end{aligned} \tag{S11}$$

where $\rho \equiv T^-(i)/T^+(i) = 1 - s$, and we have used the fact that

$$\begin{aligned} T^+(i) &= \frac{i(N-i)}{N - s(N-i)} \\ T^-(i) &= \frac{i(N-i)(1-s)}{N - s(N-i)}. \end{aligned} \tag{S12}$$

Equation S11 is a second order linear difference equation with constant coefficients. It has general solution $p_i = c_1 + c_2\rho^i$, and given the boundary conditions $p_0 = 0$ and $p_N = 1$, we can solve for the constants c_1 and c_2 to arrive at

$$p_i = \frac{1 - \rho^i}{1 - \rho^N}. \tag{S13}$$

For $i = 1$ and $\rho = 1 - s$, we therefore have

$$P_{fix}(s) \equiv p_1 = \frac{s}{1 - (1-s)^N}. \tag{S14}$$

7 Analytical Approximation for Multiple Habitats

To derive an approximate expression for τ_f in the $M = 3$ vial array, we again consider the limit where the arrival of the first mutant in each vial dominates

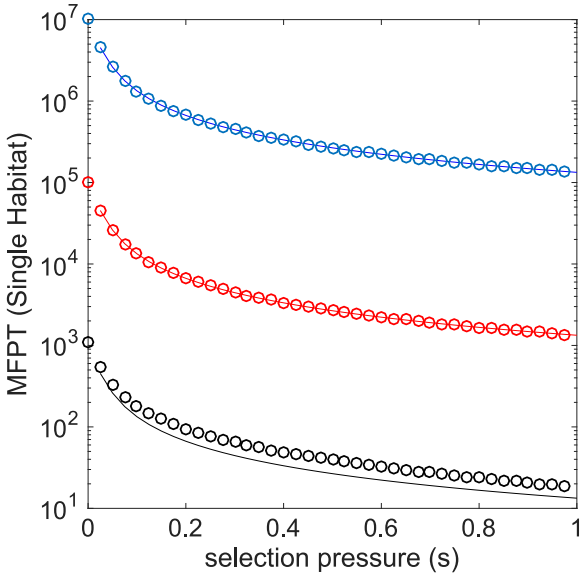

Figure S6: Within a single vial system, the fixation time is well-approximated for sufficiently small μ by Equation S10. Circles: exact calculation; solid line: approximation. Mutation rates are $\mu = 10^{-7}$ (blue), $\mu = 10^{-5}$ (red), and $\mu = 10^{-3}$ (black). $N = 75$ for all curves. Fixation times are measured in units of N^{-1}.

the fixation time, which now corresponds to $\mu, \beta \ll 1$. In this limit, the time to fixation within a single vial—given the presence of a single initial mutant—is again fast compared to the arrival time of that first mutant, which now can be due to either a mutation event (at rate μN) or a migration event (at rate $N\beta n_{fix}$, where n_{fix} is the integer number of (connected) neighboring vials that have already achieved fixation). Therefore, the different habitats effectively achieve fixation one at a time, and the fixation time within each vial is an exponential process governed by a rate

$$\lambda(s, n_{fix}) = N(\mu + \beta n_{fix}) P_{fix}(s) \tag{S15}$$

with $P_{fix}(s)$ again given by Equation S14. For economy of notation, we introduce the shorthand $\lambda_i(n_{fix}) \equiv \lambda(s(x_i), n_{fix})$. The global fixation time, which depends on the distribution of selection pressures in the three habitats, can be approximated by

$$\tau_f \approx \tau_{min} + Q(x_0)\tau^{\beta}_{max}(x_1, x_2) + Q(x_1)\tau^{\beta}_{max}(x_0, x_2) + Q(x_2)\tau^{\beta}_{max}(x_0, x_1). \tag{S16}$$

τ_{min} is the fixation time of the fastest vial in the absence of migration and is given by the expected minimum of three independent, exponentially distributed variables with rates $\lambda_i(0)$,

$$\tau_{min} = \frac{1}{\lambda_0(0) + \lambda_1(0) + \lambda_2(0)}. \tag{S17}$$

$Q(x_i)$ is the probability that the vial at location x_i was the first to reach fixation in the absence of migration, and it is given by

$$Q(x_i) = \frac{\lambda_i(0)}{\sum_{j=0}^{2} \lambda_j(0)} \tag{S18}$$

The β dependence of Equation S16 is contained in the terms $\tau^{\beta}_{max}(x_i, x_j)$, which also implicitly contain information about the connection topology. $\tau^{\beta}_{max}(x_i, x_j)$ is the expected maximum time of two independent fixation events occurring in habitats x_i and x_j, assuming that the third habitat ($x_k \neq x_i, x_j$) has already achieved fixation and can therefore supply seed mutants at a rate βN. For example, we have

$$\tau^{\beta}_{max}(x_0, x_1) = \frac{1}{\lambda_0(0) + \lambda_1(1)} + \frac{\lambda_0(0)}{\lambda_0(0) + \lambda_1(1)}(\lambda_1(2))^{-1} + \frac{\lambda_1(1)}{\lambda_0(0) + \lambda_1(1)}(\lambda_0(1))^{-1} \tag{S19}$$

where the first term is the expected minimum time of two independent processes occurring at rates $\lambda_0(0)$ and $\lambda_1(1)$; note that since the vial at x_2 has already achieved fixation, the rate for the vial at x_1 is taken at $n_{fix} = 1$, which accounts for migration from vial x_2 to x_1. The second term in Equation S19 is a product of two terms: the probability that the vial at x_0 achieves fixation before the vial at x_1, and the rate at which the vial at x_1 would achieve fixation ($1/\lambda_1(2)$). The latter rate corresponds to $n_{fix} = 2$, as vials at x_0 and x_2 have already

achieved fixation and can both contribute βN to the arrival rate of the first mutant. Finally, the last term is a product of two terms: the probability that the vial at x_1 achieves fixation before the vial at x_0, and the rate at which the vial at x_0 would achieve fixation ($1/\lambda_0(1)$).

Because of the symmetry of the selection pressure profiles considered here ($s(x_0) = s(x_2)$), we have $\tau^{\beta}_{max}(x_0, x_1) = \tau^{\beta}_{max}(x_1, x_2)$, while the remaining term in Equation S16 is given by

$$\begin{aligned}\tau^{\beta}_{max}(x_0, x_2) &= \frac{1}{\lambda_0(1) + \lambda_2(1)} + \frac{\lambda_0(1)}{\lambda_0(1) + \lambda_2(1)}(\lambda_2(1))^{-1} + \frac{\lambda_2(1)}{\lambda_0(1) + \lambda_2(1)}(\lambda_0(1))^{-1} \\ &= \frac{3}{2\lambda_0(1)}\end{aligned} \tag{S20}$$

where the last line accounts for the symmetry of the selection profile.

By combining Equation S16 with Equations S14, S15, and S17-S20, we arrive at a general equation for τ_f that depends on the selection pressure profile, μ, β, and N. The general expression is long and cumbersome, but it is straightforward to numerically evaluate τ_f for any value of the parameters. We find that the approximation performs surprisingly well over a large range of parameter values, qualitatively reproducing all features of the full MFPT calculation (Figure S7, main panel; Compare to Figure 2, main text) and even providing excellent quantitative agreement in many cases (Figure S7, bottom panels). To gain additional analytical insight into the model, we consider in what follows several limiting cases where additional analytical progress is tractable.

7.1 $\beta \ll \mu$ Limit

To investigate the limit $\beta \ll \mu$, we expand Equation S16 in the small parameter $\epsilon_1 \equiv \beta/\mu$ and neglect terms of order ϵ_1 and higher. In this limit, τ_f in Equation S16 reduces to τ_{max}, given by

$$\tau_{max} = \frac{2}{\lambda_0(0)} + \frac{1}{\lambda_1(0)} - \frac{2}{\lambda_0(0) + \lambda_1(0)} - \frac{1}{\lambda_0(0) + \lambda_2(0)} + \frac{1}{2\lambda_0(0) + \lambda_1(0)}, \tag{S21}$$

which is the expected maximum of three independent exponentially distributed random variables; note that we have again taken into account the symmetry in the selection pressure profile ($\lambda_0 = \lambda_2$). In this limit, the three vial system acts effectively as three independent systems, with the overall fixation time corresponding to the slowest fixation. After rewriting τ_{max} in terms of $\langle s \rangle$ and δs, it is straightforward (though algebraically tedious) to show that $(\partial \tau_{max}/\partial \delta s)|_{\delta s=0} = 0$ and $(\partial^2 \tau_{max}/\partial \delta s^2)|_{\delta s=0} > 0$, indicating that the homogeneous landscape ($\delta s = 0$) minimizes the fixation time, consistent with results of the exact calculation. Intuitively, increasing heterogeneity reduces the minimum selection pressure in the spatial array, which in turn slows the expected maximum fixation time among the three habitats.

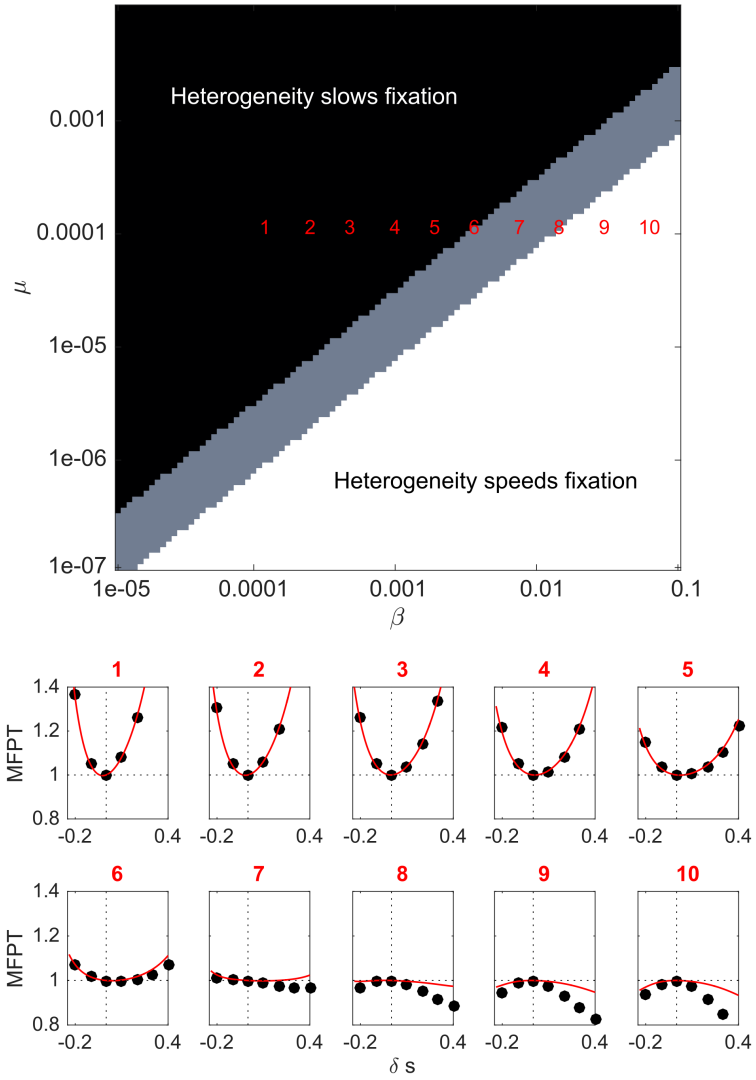

Figure S7: Parameter regimes and fixation time curves calculated using approximate MFPT (compare to Figure 2, main text). MFPT approximations were performed for the indicated values of β and μ and for $-0.2 \leq \delta s \leq 0.5$ in steps of 0.025. Red numbers on the main plot correspond to curves shown in the subplots below. Black circles: exact calculation. Red curves: approximation.

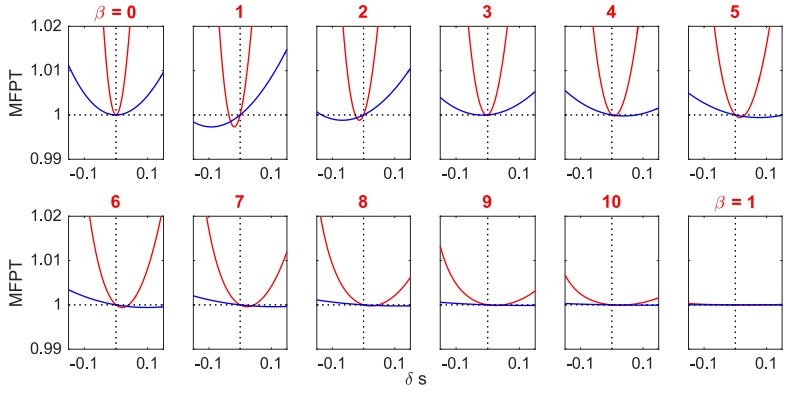

Figure S8: Fixation times near the origin as a function of δs in the $N \to \infty$ limit. β and μ values for panels labeled 1-10 are the same as in Figure S7; we've also included $\beta = 0$ and $\beta = 1$. $\langle s \rangle = 1/6$ (red) and $\langle s \rangle = 5/6$ (blue).

7.2 $\beta \gg \mu$ Limit

To investigate the limit $\beta \gg \mu$, we expand Equation S16 in the small parameter $\epsilon_2 \equiv \mu/\beta$. The dominant term is of order $1/\epsilon_2$, and we ignore terms of order unity and higher. In the limit $\beta \gg \mu$, τ_f in Equation S16 reduces to the expected minimum of three independent exponential processes, leading to $\tau_f \approx \tau_{min}$ (Equation S17). In this limit, the fixation time is dominated by dynamics in the vial that first achieves fixation; the remaining vials then rapidly achieve fixation due to fast migration. For large but finite N, the fixation time τ_{min} is maximized at $\delta s = 0$, indicating that heterogeneity always accelerates fixation, again consistent with the exact calculation (Fig. 2b, right panel). In this limit, the effective rate of fixation λ_{eff} is increased for all $\delta \neq 0$, as heterogeneity decreases fixation time in the vial with the fastest average fixation.

7.3 Large N Limit

While our primary focus is on finite populations, we briefly consider here the limit of $N \to \infty$, where Equation S16 reduces (after simplification) to

$$\tau_f^{\infty} \approx \frac{1}{\mu(2s_0 + s_1)} \left[1 + \frac{3\mu s_1}{2(\beta + \mu)s_0} + \frac{2\mu \left(2\beta s_1(s_0 + s_1) + \mu(s_0^2 + s_0 s_1 + s_1^2) \right)}{(2\beta + \mu)s_1(\beta s_1 + \mu(s_0 + s_1))} \right] \tag{S22}$$

Note that prior to taking the $N \to \infty$ limit, we first rescaled our time units by a factor of N. We've also used the shorthand $s_i \equiv s(x_i)$ and consider only symmetric landscapes ($s_0 = s_2$).

In the limit $s_1/s_0 \to 0$ (large selection valley), Equation S22 reduces to $\tau_f^{\infty} = 1/(s_1(2\beta + \mu))$, which corresponds to selection in a single vial of selection pressure s_1 where seed mutants can arise due to mutation (μ) or due to migration

from one of two vials that have already achieved fixation (2β). Fixation in the center vial is the rate limiting step for global fixation. Similarly, when $s_0/s_1 \to 0$ (large selection peak), we have $\tau_f^\infty = 3/(2s_0(\beta+\mu))$, which is the maximum of two independent exponential processes that each occur at rate $s_0(\beta+\mu)$. Fixation in the peripheral vials is the rate-limiting process.

To evaluate the magnitude of the change in fixation time as the selection profile is modulated, we fix the average selection pressure $\langle s \rangle$ and calculate the difference in fixation times $\Delta\tau$ between a selection profile with a large peak ($s_0 = s_2 \sim \epsilon_0$) and one with a large valley ($s_1 \sim 2\epsilon_0$), where $\epsilon_0 \ll 1$ is assumed to be small so that the vast majority of the selection pressure is concentrated either in the center vial or the edge vials. By expanding Equation S22 in ϵ_0 and ignoring terms of order ϵ_0 or higher, we have

$$\frac{\Delta\tau}{\tau_v} = \frac{\tau_p - \tau_v}{\tau_v} = \frac{5+2\gamma}{1+\gamma} > 0, \tag{S23}$$

where τ_v (τ_p) corresponds to the selection profile with a large valley (peak) and $\gamma \equiv \mu/\beta$. The fixation time is always larger (slower) in a sharply peaked landscape than one with a sharp valley. Choosing the peaked landscape over the valley leads to a relative increase of 2-5 fold depending on the ratio of mutation to migration.

Following a change of variables in Equation S22 from $\{s_i\} \to \langle s \rangle$ and δs, we find that the homogeneous landscape is an optimum ($(\partial\tau_f^\infty/\partial\delta s) = 0$) only for $\beta = 0$ and $\beta = \mu\left(7+\sqrt{145}\right)/4$, and each corresponds to a minimum of the fixation time. Surprisingly, then, all other values of β correspond to the intermediate regime, where heterogeneity can either slow or speed fixation depending on the specific landscape. In practice, the value of δs for which a minimum occurs is often very close to zero, though it does depend on $\langle s \rangle$ (Figure S8). Large heterogeneity–either a peak ($\delta s > 0$) or a valley ($\delta s < 0$)–tends to slow fixation. For $\beta \gg \mu$, the fixation time reduces to $\tau_f^\infty \approx (3\mu\langle s \rangle)^{-1}$ and no longer depends on δs; this corresponds to the fixation time of a single habitat with effective selection pressure $s_e = 3\langle s \rangle$, where the factor of 3 results from a tripling of the population size (relative to a single vial).

7.4 Time to Fixation With Initial Mutants

We now consider the case when there are $N/2$ resistant mutants in the middle habitat (x_1). In this case, we can approximate the time to fixation $\tau_f^{N/2}$ as

$$\tau_f^{N/2} \approx [P_{fix}(s_1, N/2)]\tau_{max}^\beta(x_0, x_2) + (1 - P_{fix}(s_1, N/2))\tau_f \tag{S24}$$

where $\tau_{max}^\beta(x_0, x_2)$ is given by Equation S20, τ_f is the fixation time starting from zero initial mutants (Equation S16), and $P_{fix}(s, N/2)$ is the probability of fixation in a single vial with selection pressure s starting from $N/2$ initial mutants,

$$P_{fix}(s, N/2) = \frac{1-(1-s)^{N/2}}{1-(1-s)^N}. \tag{S25}$$

The first term in Equation S24 corresponds to the middle vial achieving fixation first, while the second term corresponds to another vial first achieving fixation. As before, we are assuming sufficiently small μ and β that the fixation (or extinction) of a mutant population in a single vial happens much faster than the typical arrival time of a new mutant via migration or mutation. In the limit $N \to \infty$, the middle vial is guaranteed to reach fixation first, and Equation S24 reduces to $\tau_f^{N/2} = 3/(2s_0(\beta+\mu))$, which is the expected maximum of the (independent) fixation times for the edge vials. In this limit, it is always optimal to distribute the drug in the habitats with no initial mutants (i.e. minimize s_0).

For general N, fixation in the middle habitat is not guaranteed, and the optimal strategy will depend on μ and β. While Equation S24 is a cumbersome expression that depends nonlinearly on the system parameters, it is easy to evaluate numerically, and we find that it provides an excellent approximation to the exact results in the parameter regimes considered here (Figure 3b-d).